論文内容の要旨

論文題目 Stepwise Construction of Metal Complex Wires on Hydrogen-Terminated Silicon Surface and Their Electrochemical Evaluations

（水素終端化シリコン表面における金属錯体ワイヤの逐次的構築と電気化学的評価）

氏名　前田　啓明

Introduction

In resent researches, the formation of self-assembled monolayers (SAMs) and molecular multilayers on metal electrodes has attracted intense attention as an effective method to construct nanoscale structures. The stepwise coordination method is one of the most significant techniques to fabricate molecular multilayer structures on an electrode modified with SAMs because it allows us to construct metal complex oligomer wires of desired structures by simple processes, and to introduce various metal ions and functional ligand molecules. In this decade, various metal complex wires have been fabricated, and their electron transport properties and conductivity have been evaluated on metallic substrates. However, most of present electric devices rely on semiconducting materials such as silicon. Therefore, the evaluation of electric properties for SAMs on semiconducting electrodes is the next target in order to make molecular electronics come true.

In the present study, $Fe(tpy)_2$ (tpy = 2,2':6',2''-terpyridine) complex wires were fabricated on hydrogen-terminated silicon(111) electrode by the hydrosilylation reaction and the stepwise coordination method. Their electron transport properties were evaluated by the electrochemical measurements.

Quantitative evaluation of the anchor ligand effect on the electron transfer rate constant

In order to realize high-performance molecular electronic devices, the rapid electron transport between an electrode and a molecular system is required. The electrode-molecular junction plays an important role in the electron transport behavior. Therefore, it is expected that the knowledge about the relationship between the electron transfer rate constant (k_{ET}) and an anchor molecule contributes to the achievement of molecular devices. In this research, $Fe(tpy)_2$ complexes

were immobilized on semiconducting silicon electrode via various linker structures, and their k_{ET} values were estimated. The effect of molecular junctions on the electron transport was investigated.

The Fe(tpy)$_2$ complexes, Si-**A**^{x}**FeL** (x = 1 − 4), were fabricated on hydrogen-terminated silicon(111) surfaces by the stepwise coordination method (Figure 1). The complexes were immobilized by the covalent Si-C bond when **A**^{1} and **A**^{2} were chosen as anchor ligands while **A**^{3} and **A**^{4} gave the Si-O-C bond. **A**^{2} and **A**^{4} contain a phenylene bridge in their structure. The modified electrodes were characterized by means of cyclic voltammetry (CV), X-ray photoelectron spectroscopy (XPS) and atomic force microscopy (AFM). In CV measurements, all samples showed the reversible redox waves derived from $[Fe(tpy)_2]^{3+/2+}$, and their proportional relationship between the peak current and scan rate suggested that these redox peaks originate from the surface confined species. In XP spectra, the peaks of Fe 2p, N 1s, and F 1s (contained as counter anion BF_4^-) were observed in all samples. These results suggest that Fe(tpy)$_2$ complexes were fabricated on H-terminated silicon electrodes.

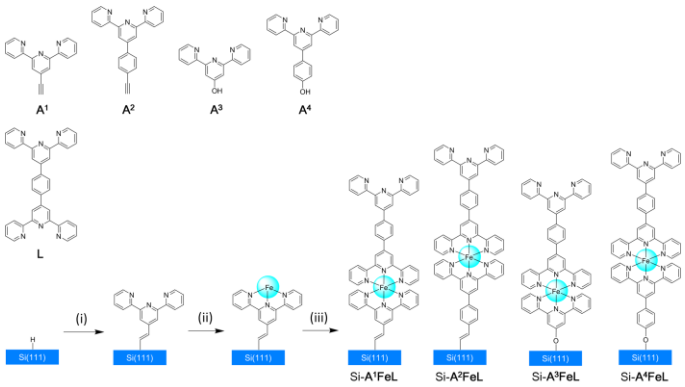

Figure 1. Structures of ligands (**A**^{x}, x = 1 – 4, **L**) and Fe(tpy)$_2$ complexes on H-terminated Si surfaces, and the stepwise fabrication process of Fe(tpy)$_2$ complex, (i) modification with anchor ligand, (ii) coordination of Fe^{2+}, and (iii) coordination of **L**.

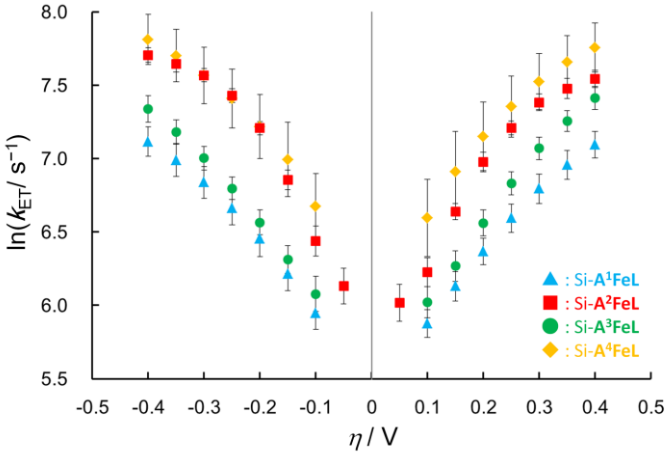

Figure 2. Tafel plots (ln k_{ET} *vs.* overpotential, η) for Si-**A**^{1}**FeL** (blue triangles), Si-**A**^{2}**FeL** (red squares), Si-**A**^{3}**FeL** (green circles), and Si-**A**^{4}**FeL** (orange diamonds).

The estimation of k_{ET} values was performed by potential step chronoamperometry (PSCA). The Fe(tpy)$_2$ complexes linked by the anchor ligands containing a phenylene unit (**A**^{2} and **A**^{4}) showed greater k_{ET} values than those of Si-**A**^{1}**FeL** and Si-**A**^{3}**FeL** in spite of their longer distance between the silicon electrode and redox center (Figure 2). The molecular orbitals estimated by DFT calculation using the simplified structures (Si-**A**^{x}**Fetpy**, x = 1 − 4) disclosed that those molecules have HOMO−3 which is delocalized over the whole molecular system, thereby contributing to the electron transport. In comparison of the energy gaps between HOMO and HOMO−3, those of Si-**A**^{2}**Fetpy** and Si-**A**^{4}**Fetpy** were smaller than those of Si-**A**^{1}**Fetpy** and Si-**A**^{3}**Fetpy**. This smaller energy difference in Si-**A**^{2}**FeL** and Si-**A**^{4}**FeL** gave a rapid electron transport behavior.

Comparison of the electron transport ability between vinylene bridge and phenylene bridge

In our laboratory, the new Pd-catalyzed modification method for hydrogen-terminated silicon surface was developed. It allows us to prepare a uniformed SAM on surface with the direct silicon-arene bond, and it is expected that this

connection can produce the greater electron transfer than the vinylene bridge formed by the traditional hydrosilylation reaction. The $Fe(tpy)_2$ complex Si-**A^{5}FeL** was prepared on silicon surface, and its k_{ET} value was estimated by PSCA. From the comparison with Si-**A^{1}FeL**, the effect of phenylene bridge and vinylene bridge on the electron transfer was evaluated. The calculated k_{ET} value for Si-**A^{5}FeL** was greater than that of Si-**A^{1}FeL** (Figure 3). Therefore the Si-**A^{5}FeL** has the superior electron transportability than Si-**A^{1}FeL**. According to the molecular orbital energy obtained by the DFT calculation, the energies of HOMO, HOMO−1 and HOMO−2 for Si-**A^{1}Fetpy** and Si-**A^{5}Fetpy** are almost constant while the HOMO−3 energy level for Si-**A^{5}Fetpy** rises 0.18 eV from that of Si-**A^{1}Fetpy** due to the expansion of π-conjugation by phenylene bridge. Hence, the small energy difference between HOMO and HOMO−3 achieved in Si-**A^{5}FeL**, and exhibited the greater electron transfer than Si-**A^{1}FeL**.

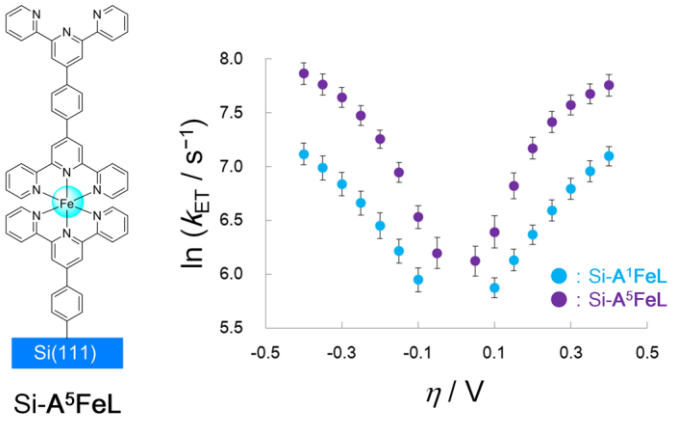

Figure 3. Structure of Si-**A^{5}FeL** and Tafel plots for Si-**A^{1}FeL** (blue circles) and Si-**A^{5}FeL** (purple circles).

Electron transport behavior of multilayered $Fe(tpy)_2$ wires on silicon electrode

The $Fe(tpy)_2$ complex multilayer wires terminated by ferrocene unit (**T^1**) and triarylamine moiety (**T^2**) (Si-**A^2(FeL)$_{n-1}$FeT^x**) were prepared by the sequential complexation method (Figure 4). The surface coverage values of $Fe(tpy)_2$ were calculated from the cyclic voltammograms increased with an increase in the number of the layers. This sequence of results suggests that the metal complex wires were elongated in a layer-by-layer fashion. In the case of Si-**A^2(FeL)$_{n-1}$FeT^1**, the reversible redox wave derived from **T^1** was observed at low scan rates. However, when the scan rate was increased, the peak separation between the oxidation and reduction wave (ΔE_p) increased from 0.031 ± 0.005 V at 25 mVs^{-1} to 0.13 ± 0.01 V at 1000 mVs^{-1} (n = 1), and the peak shape become broader (Figure 5(A)). This behavior suggests that the electron transport between electrode and **T^1** is slow even in the case of short wires. On the other hand, **T^2** showed a reversible redox wave at high scan rates in the 3-layer wire (Figure 5(B)), and its ΔE_p value was 0.021 ± 0.002 V at 1000 mVs^{-1} (n = 3). This behavior indicates that the electron transport between electrode and **T^2** is much faster than the case of **T^1**. This difference of electron transport behaviors can be explained by the energy diagram of silicon and molecular wires. The vacuum energy levels of HOMO for ferrocene, the conduction band edge and

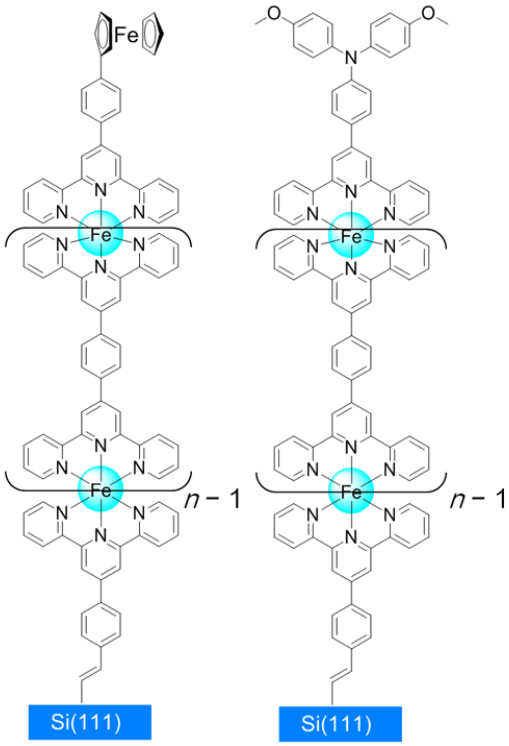

Figure 4. Structures of Si-**A^2(FeL)$_{n-1}$FeT^1** (left) and Si-**A^2(FeL)$_{n-1}$FeT^2** (right).

valence band edge of silicon are − 4.8 eV, − 4.05 eV and − 5.17 eV respectively. From these values, the HOMO energy levels for $Fe(tpy)_2$ complex, $\mathbf{T^1}$ and $\mathbf{T^2}$ can be expressed in accordance with the redox potentials estimated from CV (Figure 6). When the redox reaction of $\mathbf{T^1}$ occurs, the valence band is filled with electrons, and the band edge is bent to get the Fermi level of silicon electrode lined up to the HOMO level of the ferrocene moiety. In this situation, the electron transported via the energy level of $Fe(tpy)_2$ is prevented from being injected in the valence band due to two factors. One is the occupied valence band and the other is the large potential barrier. They make it difficult to introduce electrons to the electrode. In the case of $\mathbf{T^2}$, its redox potential is close to the energy level of the valence band edge and $Fe(tpy)_2$ redox potential. In this situation, the deformation of the band edge is smaller than the case of $\mathbf{T^1}$. In addition, it is considered that a part of the $Fe(tpy)_2$ units can be oxidized because the applied potential is close to the redox potential of $Fe(tpy)_2$ complex, and they can work as a pathway of electrons from the terminal redox species. Therefore, $\mathbf{T^2}$ showed the reversible redox reaction.

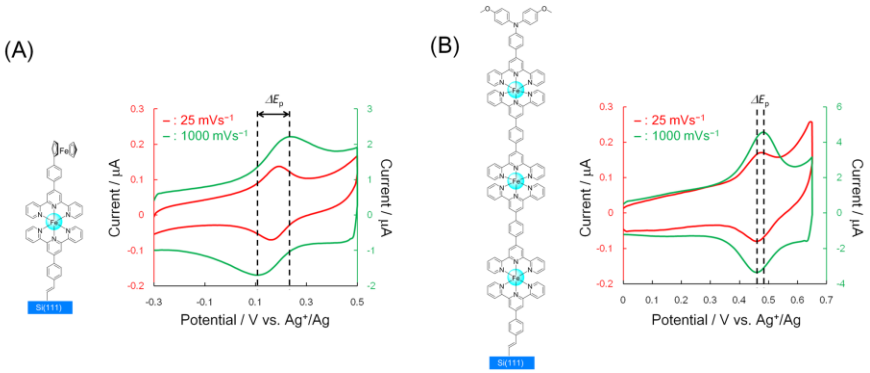

Figure 5. Cyclic voltammograms of terminal redox moieties: (A) $\mathbf{T^1}$ in Si-$\mathbf{A^2FeT^1}$ at 25 mVs^{-1} (red solid line) and 1000 mVs^{-1} (green solid line), and (B) $\mathbf{T^2}$ in Si-$\mathbf{A^2(FeL)_2FeT^2}$ at 25 mVs^{-1} (red solid line) and 1000 mVs^{-1} (green solid line).

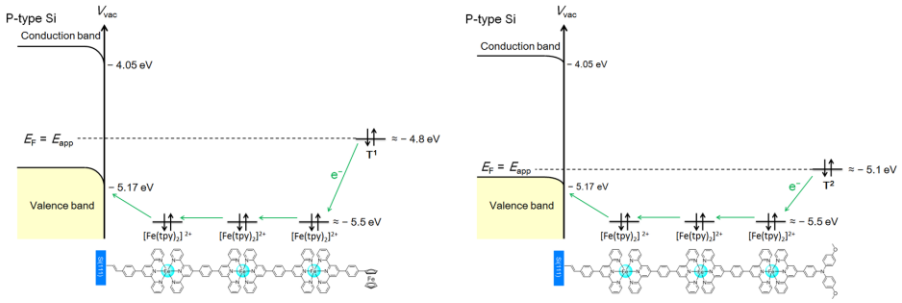

Figure 6. Estimated energy diagrams for Si-$\mathbf{A^2(FeL)_{n-1}FeT^x}$ applied same potential with the HOMO energy levels of terminal ligands, and the electron transport pathways from $\mathbf{T^x}$.

Conclusion

In the series of research, the $Fe(tpy)_2$ molecular wires were fabricated on hydrogen-terminated silicon(111) electrode and their electron transport properties were quantified. The $Fe(tpy)_2$ complexes linked via the phenylene-containing anchors exhibit greater k_{ET} values due to the existence of the molecular orbitals assist the electron transfer. In addition, $\mathbf{A^5}$ linked on silicon via the direct Si-aryl bond improved the electron transfer. The ferrocene moiety at the termini of multilayered wires showed a large peak separation, indicating slow electron transport. On the other hand, $\mathbf{T^2}$ afforded a reversible redox couple, or fast electron transfer. This phenomenon can be explained by the relationship among the energy level of the silicon electrode, terminal redox species, and $Fe(tpy)_2$ complex.